ELSEVIER

Earth and Planetary Science Letters 203 (2002) 1059–1071

EPSL

www.elsevier.com/locate/epsl

Ground surface temperature histories inferred from deep borehole temperature–depth data in Eastern Siberia

R.P. Dorofeeva [a,*], P.Y. Shen [b], M.V. Shapova [a]

[a] Institute of the Earth's Crust, Siberian Branch of the Russian Academy of Sciences, Lermontov Str. 128, Irkutsk 664033, Russia
[b] Department of Earth Sciences, University of Western Ontario, London, ON, Canada N6A 5B7

Received 29 May 2002; received in revised form 16 August 2002; accepted 16 August 2002

Abstract

Temperature–depth data from 14 deep boreholes, located in the Irkutsk amphitheater and Baikal rift zone in Eastern Siberia, have been used to infer ground surface temperature (GST) histories for the last 100 ka. The results show that the estimated small-scale and recent GST changes and the long-term mean have been significantly contaminated by the presence of drilling disturbances. On the other hand, large-scale features, such as the Pleistocene/Holocene (P/H) transition, appear to have been adversely affected to a much lesser extent, as suggested by the internal consistency of the inverse results. The estimated GST histories exhibit a pattern of north to south variation, with the P/H warming varying from about 25 K at a latitude of 56°N to less than 8 K at 54°N and then back to 25 K at 52°N. The timing and duration of the transition also vary. In the north, warming began as early as 90 ka and reached a maximum at about 7 ka, and in the south, warming did not begin until about 20 ka and reached a maximum at about 4 ka.

Keywords: paleoclimatology; Siberia; ground surface temperature; borehole temperature; inversion

1. Introduction

Global climatic warming and its role in the general framework of ecological risk have, in recent years, become a problem of paramount importance [1]. One aspect of the problem, which is being intensively studied, concerns the relative roles of natural variability and anthropogenic influence in the recent warming. This, in turn, motivates the reconstruction of past climate changes from proxy data since instrumental records are typically available for only the past 150 years or so. Traditional proxy reconstructions use records such as tree rings, ice and sediment cores, and corals [2–5]. In this work, we consider geothermal reconstruction. Subsurface temperature–depth (*T*–*z*) data obtained in boreholes comprise an independent archive of past surface temperature changes, which is complementary to both the instrumental and the traditional proxy records. Geothermal reconstructions with a global coverage include [6–8]; readers are referred to referen-

* Corresponding author. Tel.: +7-395-2-426900; Fax: +7-395-2-462900.

E-mail addresses: drf@crust.irk.ru (R.P. Dorofeeva), pys@uwo.ca (P.Y. Shen).

0012-821X/02/$ – see front matter © 2002 Elsevier Science B.V. All rights reserved.
PII: S0012-821X(02)00925-1

ces cited therein for other reconstructions of regional scales. Most of these studies focus on the estimation of ground surface temperature (GST) histories for the past 500–1000 years, in part because this period is the most relevant in extending the instrumental records to pre-industrial periods [8] but also in part because most of the T–z data sets are obtained in boreholes that are less than 600 m in depth, which carry little information about GST changes prior to 1 ka.

In this work, we attempt the reconstruction of GST histories over a much longer period, in the order of 100 ka to 1 Ma, using T–z data obtained from deep boreholes. The area studied is shown in Fig. 1. It consists of part of the Irkutsk amphitheater (south of the Siberian platform) and part of the Baikal rift zone. Data from 14 boreholes in total are available, and except for Belskaya-1 and Birkinskaya-2, the boreholes are all sufficiently deep to allow for at least a partial resolution of the Pleistocene/Holocene (P/H) transition. Our principal objective is to examine the spatial variability of the transition, in terms of its timing and amplitude. For very deep boreholes (>3000 m), temperatures at the last glacial maximum (LGM) may also be estimated. The presence of drilling disturbances introduces artifacts in the estimated GST histories. However, large-scale features, such as the P/H transition, remain resolvable, as suggested by the inverse results. GST changes for the most recent 500 years and the long-term mean GST, on the other hand, are not resolved because they have been significantly contaminated by the presence of drilling disturbances. For a discussion of recent GST changes in this region, readers are referred to [9].

2. Methodology

2.1. The forward model

To infer climate changes during the Pleistocene and Holocene from T–z data measured in deep boreholes, we use the functional space inverse (FSI) formulation [10,11], with the GST histories modeled as an arbitrary function of time. The theoretical T–z profile is computed from GST history on the basis of the theory of 1-D heat conduction in a laterally homogeneous Earth, using Galerkin finite element model and Crank–Nicolson finite difference scheme in the spatial and temporal domains, respectively. To ensure that GST signals from the deepest boreholes are recoverable and not erroneously telescoped into a small time interval, we set the time origin at 1 Ma, prior to which the GST may be assumed to be constant and equal to the long-term mean, and we set the base of the finite element spatial grid at 20 km to ensure that temperature perturbations due to GST changes in the past 1 Ma become insignificant at this depth. The thermal regime is completely governed by six model parameters: the transient component of the GST history ($V_s(t)$), the steady-state component of the GST history (U_s), basal heat flow density (HFD, Q_b), thermal conductivity ($K(z)$), heat capacity per unit volume ($\rho C(z)$), and rate of heat production ($A(z)$). During inversion, the six model parameters are simultaneously estimated from the T–z data.

2.2. Constraining the GST history

In the framework of the FSI formulation, a crucial consideration is the choice of the a priori autocovariance for $V_s(t)$ [11,12]. Because non-climatic factors, such as the presence of drilling disturbances, are not included in the thermal model, their effects must be treated as noise to be suppressed or minimized in the inversion. If the noise is gaussianly distributed, we can effectively suppress its adverse effects by appropriately relaxing the constraint imposed on the T–z data at the cost of also muting to some extent the genuine GST signals. However, the effects of drilling disturbances are likely to be systematic and as such cannot readily be suppressed in this manner. An exception is when the signature of the drilling disturbances differs significantly from that of the sought-after climatic signals. In this case, we can suppress the adverse effects by imposing an a priori autocovariance for $V_s(t)$ that caters to the signature of the climatic signals. In this work, after extensive numerical experiments with synthetic data, we choose an a priori autocovariance for $V_s(t)$ in the form of V_s(5–2 K, 50 000–100 yr)

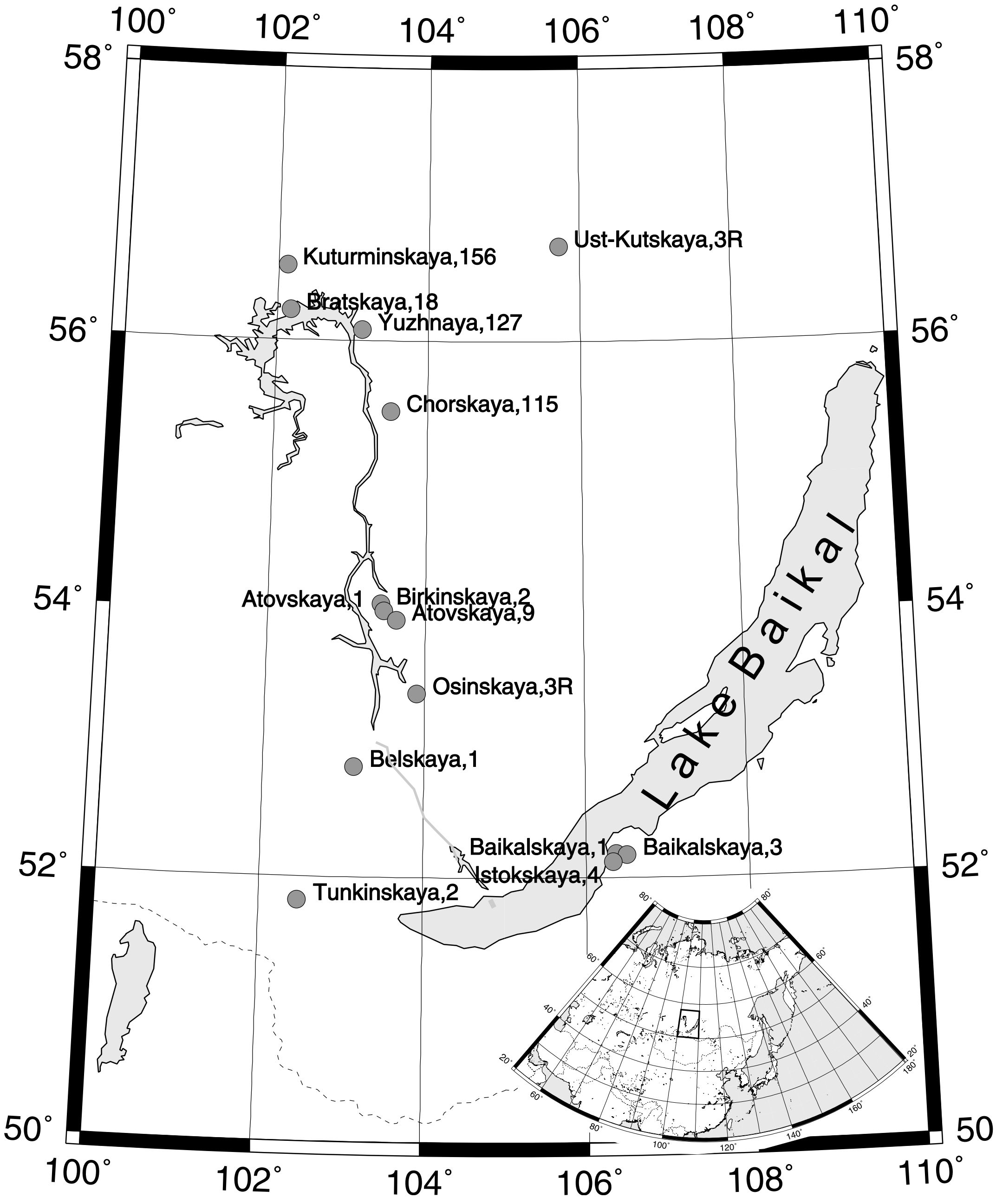

Fig. 1. Map of the studied area in Eastern Siberia, showing borehole sites used in this work.

for the time period of (0.1 Ma, now). We focus on the last 0.1 Ma because this is the time period for which the T–z data contain significant information about the GST changes. The chosen autocovariance specifies that $V_s(t)$, or more precisely the deviation of $V_s(t)$ from its a priori value (which is set to zero to avoid bias), has a Gaussian autocovariance with standard deviation (S.D.) varying linearly from 5 K at 0.1 Ma to 2 K at now, and with correlation time varying linearly from 50 000 yr at 0.1 Ma to 100 yr at now. Specifying a correlation time that increases linearly with elapsed time is consistent with the finding that the extent of spreading of GST signals due to diffusion is roughly proportional to the time elapsed [13]. In other words, the specified correlation time will not unduly suppress genuine GST signals, but will be effective in suppressing non-climatic factors with different correlation time scales. Specifying a linearly increasing S.D. with the elapsed time is not an unbiased choice. The unbiased choice would be a time-independent S.D. However, a linearly increasing S.D. facilitates the recovery of early GST changes. There are two plausible choices for the settings of S.D. and correlation time prior to 0.1 Ma. The optimistic choice is to continue the linear extrapolation such that the S.D. and correlation time at 1 Ma are 32 K and 500 000 yr, respectively. These settings would favor the recovery of even the faintest long-period GST signals that may be present in the data, but also at the risk of enhancing the artifacts of noise. We opt for the more conservative choice by setting the S.D. and correlation time prior to 0.1 Ma to constants equal to their respective values at 0.1 Ma. The conservative settings are strong enough to constrain the GST to taper to the long-term mean at 1 Ma in most cases. For the boreholes studied in this work, GST histories inferred with autocovariance functions that differ in the time period of (1, 0.1 Ma) are virtually identical between 0.1 Ma and now, but may diverge as we go back further in time, reflecting the fact that the *T*–*z* data do not constrain GST changes prior to 0.1 Ma.

2.3. Constraining *T*–*z* and *K*–*z* data

Once the a priori autocovariance for $V_s(t)$ has been chosen, the inverse solution depends largely on the extent to which *T*–*z* and *K*–*z* (thermal conductivity–depth) data are constrained [11,12,14–16]. If the thermal regime is properly modeled, the a priori S.D.s for *T*–*z* and *K*–*z* data should be assigned values in accordance with the actual levels of measurement errors. In this work, however, the assignment of the a priori S.D.s must also account for systematic noise that arises from non-climatic factors, such as the presence of drilling disturbances. There are two plausible strategies for suppressing the artifacts of systematic noise. One strategy is to over-relax the constraints on *T*–*z* data, i.e., to assign a priori S.D.s larger than the measurement errors. The other is to over-relax the constraints on *K*–*z* data. For the retrieval of short-term and recent GST changes over the past 1000 years, the superior strategy was to over-relax the constraints on *K*–*z* data [14]. However, the strategy works poorly for the retrieval of long-term GST changes because perturbations to the subsurface *T*–*z* profile caused by long-term GST changes are generally indistinguishable from those caused by systematic *K*–*z* variations. Over-relaxing the constraints on *K*–*z* data would therefore tend to misinterpret genuine GST signals as systematic *K*–*z* variations. The superior strategy for retrieving long-term GST changes is to over-relax the constraints on *T*–*z* data [15,16]. In this work, we take the strategy further by treating the *K*–*z* profile as perfectly known so that the artifacts of noise are to be suppressed by over-relaxing the constraints on *T*–*z* data alone. We note that, in the Monte Carlo formulations of Dahl-Jensen et al. [17] and Mareschal et al. [18], the *K*–*z* profile is also taken as perfectly known.

2.4. Illustrative example

In processing each of the 14 borehole data sets, we use a series of values for the a priori S.D.s of the *T*–*z* data to obtain inverse solutions, from which we then select the optimal solution on the basis of the stability of the inferred GST history and the degree of misfit between the inferred and the measured *T*–*z* profiles. The a priori S.D. used to obtain the optimal solution ranges from 0.1 K for good data to 1.6 K for noisy data. The selection process is illustrated in Fig. 2, using the data set from Istokskaya-4. The upper panel shows three estimated GST histories when the *T*–*z* data are overly, optimally, and under-constrained. For the overly and under-constrained solutions, the a priori S.D.s are one half and two times, respectively, those used to obtain the optimal solution. The arrow to the left is the estimated long-term mean GST. We see that, for this borehole, the

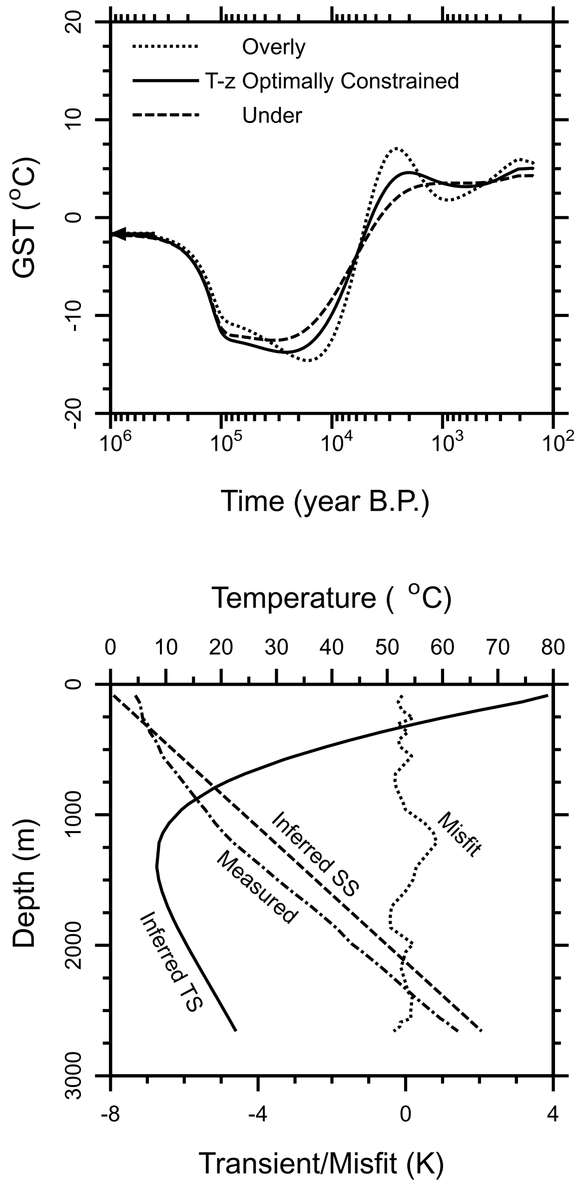

Fig. 2. (Upper panel) The estimated GST histories for Istokskaya-4 when *T–z* data are overly, optimally, and under-constrained, respectively. (Lower panel) Various *T–z* profiles for the optimal solution. See text for explanation.

inferred GST history tends asymptotically toward the long-term mean, starting at about 0.1 Ma, reflecting the fact that *T–z* data to a depth of 2659 m do not contain sufficient information about GST changes prior to 0.1 Ma. Note that GST changes for the most recent 150 years have not been plotted because this portion of the GST history is also poorly resolved due to a lack of *T–z* data in the upper 85 m of the borehole. The bottom panel of Fig. 2 shows four *T–z* profiles for the optimal solution. 'Measured' is the measured *T–z* data (upper scale), 'Inferred SS' is the estimated steady-state *T–z* profile (upper scale), 'Inferred TS' is the estimated transient *T–z* profile (lower scale), and 'Misfit' is the difference between the estimated and the measured *T–z* profiles (lower scale). We can see that a significant misfit remains in the interval of 1000–2000 m, suggesting that the full extent of the P/H transition has not been fully recovered in the optimal solution. Thus a less conservative approach would be to accept the dotted curve in the top panel as the optimal solution. In this study, we prefer to err on the conservative side and attribute the poor *T–z* fit to non-climatic factors.

The major feature of the inferred GST history for Istokskaya-4 is a P/H transition from low temperatures at the LGM to high temperatures at the Holocene maximum (HM). The transition is prominent in a majority of the inferred GST histories and will be the focus of our discussion. That the P/H transition is retrievable despite the presence of drilling disturbances can be understood by inspecting the 'Inferred TS' profile depicted in the bottom panel. The profile shows that the perturbation caused by the P/H transition is a large-scale and long-wavelength feature that cannot readily be swamped by small-scale and short-wavelength artifacts. Glacial/interglacial transitions during the Pleistocene cannot be resolved by borehole *T–z* data owing to the smoothing effect of heat conduction [13]. Climate changes following the HM cannot be reliably estimated because the artifacts of drilling disturbances may swamp genuine GST changes.

3. Data and results for Eastern Siberia

The territory of the Irkutsk amphitheater (south of the Siberian platform) is marked by a sharply continental climate with a long dry winter and abundant precipitation in summer; woods cover 67% of the area. The territory has a com-

Table 1
Coordinates, depths, altitudes and geothermal parameters of boreholes used in GSTH reconstructions

Site	Latitude/ longitude	Depth (m)	Logged interval (m)	Altitude (m)	Dates of drilling	Date of logging	Thermal conductivity (W/m/K)	Heat production (μW/m^3)	Heat flow density (mW/m^2)
Bratskaya-18	56-13/102-11	3410	55–3403	405	10.78–07.79	16.07.80	2.8	1.2	43 (43)
Chorskaya-115	55-29/103-31	3409.5	100–2480	666	1973	after 3 days	2.8	1.2	42 (49)
Kuturminskaya-156	56-33/102-07	3905	10–3878	484	08.12.78–14.01.81	30.06.80	2.8	1.2	33 (32)
Ust-Kutskaya-3R	56-42/105-43	2662	100–1828	293		17.06.53	2.8		52 (56)
Yuzhnaya-127	56-05/103-08	3338.6	100–3300	449	23.10.74–02.02.76	25.05.76	3.0	1.2	44 (50)
Atovskaya-1	54-00/103-28	2789.4	200–2770	514	20.05.57–03.10.58	12.05.58	3.0	1.3	29 (32)
Atovskaya-9	53-56/103-38	2015	75–1900	524	27.06.60–03.02.61	1966	2.9	1.3	32 (38)
Belskaya-1	52-50/103-08	1927.8	63–1443	422	07.04.48–12.10.50	16.04.50	3.2	1.3	36 (34)
Birkinskaya-2	54-03/103-26	1264	10–1055	710	31.08.64–15.11.64	1966	3.0	1.3	30 (50?)
Osinskaya-3R	53-23/103-54	2700	108–2127	415	12.06.53–24.10.56	23.09.57	3.2		45 (44)
Baikalskaya-1	52-10/106-30	1825	24–1824	468	22.08.51–14.03.53	09.07.53	2.6		52 (51)
Baikalskaya-3	52-11/106-22	2558	56–2135	463	30.06.53–14.03.54	09.07.54	2.4		50 (58)
Istokskaya-4	52-07/106-20	2802.1	85–2659	471	30.07.59–11.09.60	09.10.60	2.5		65 (68)
Tunkinskaya-2	51-49/102-28	2117	70–1996	732	10.09.53–16.02.56	21.04.56	2.4		65 (67)

plex geological structure caused by a wide development of salt tectonics and trap magmatism. Numerous boreholes were drilled in the 1950s to 1970s to search for oil and gas. Out of about 100 borehole sites for which T–z data are available, 10 have been selected for this study. Excluded are those sites for which the effects of hydrological perturbations and subsurface heterogeneity are apparent. Four other boreholes are selected from the Baikal rift zone to the south, which for some geological and geothermal parameters is distinctly different from the Irkutsk amphitheater [19]. Principal characteristics of the selected boreholes are summarized in Table 1. Relevant tectonic and lithological characteristics are summarized in Table 2. The mean thermal conductivity, mean heat production, and the heat flow density in parentheses, listed in Table 1, are used as the a priori values for $K(z)$, $A(z)$, and Q_b, respectively, in the inversion. The heat flow density in parentheses is the mean interval HFD, determined as the product of mean thermal conductivity and mean temperature gradient for various depth intervals and the un-bracketed heat flow density is the value of Q_b estimated in this work. Q_b is the basal HFD at the base (20 km) of the finite element model, assumed to be free of climatic effects. Because measurements of thermophysical properties are limited to depth intervals where oil and gas were expected, mean thermal conductivities are estimated from the lithological data given in Table 2. This poses no serious problems insofar as the P/H transition is concerned because transient perturbation due to the P/H transition is governed mainly by the mean thermal conductivity and only negligibly influenced by the detailed thermal structure. Problems would only arise if significant systematic variations exist in the thermal conductivity structure. However, systematic thermal conductivity trends are not apparent from the lithological data. For most of the selected boreholes, the largest uncertainties in the data sets come from remanent drilling disturbances. Because of industrial conditions, the boreholes could not be left unperturbed for a long period of time before being logged for temperature. A pertinent question, therefore, is whether and to what extent we can use the data to infer past climate changes. We

Table 2
Tectonic and lithological characteristics of boreholes at the south of Eastern Siberia

Tectonic unit	Name of borehole	Age	Sedimentary structure
South of the Siberian platform (Irkutsk amphitheater)			
Ust-Kutsky dome	Ust-Kutskaya-3	Q	0–24 m – sands
		€m_3–€m_1	marls, dolomites, limy dolomites, rock salt with quartz dolomite, trap intrusions
Zone of Angarsk dislocations			
Sedanovsky uplift	Kuturminskaya-156	$Q–O_1$	0–230 m – sandy deposits
		€m_3–€m_1	carbonate-terrigenous rocks (by analogy)
Bratsky uplift	Bratskaya-18	Q	0–10 m – sands and loams
		€m_3–€m_1	sandstones, argillites, dolomites, limestones, rock salt, trap intrusions
Central field of the Irkutsk amphitheater (Angarsk syneclise)			
Zayarsky uplift	Yuzhnaya-127	€m_3–€m_1	sandstones, marls, argillites, dolomites, limestones, rock salt, trap intrusions
Chorsky uplift	Chorskaya-115	€m_3–€m_1	sandstones, aleurolites, marls, dolomites, dolomitic anhydrites, limestones, rock salt, trap intrusions
Zone of Verkhneangarsk dislocations			
Birkinsky uplift	Birkinskaya-2	Q	0–2 m – loams, sandy loams
		€m_3–€m_1	sandstones, marls, rock salt, dolomites, dolomitic anhydrites
Atovsky uplift	Atovskaya-1	Q	0–5 m – sandy loams, loams
	Atovskaya-9	€m_3–€m_1	sandstones, marls, aleurolites, argillites, dolomites, dolomitic anhydrites
Osinsky uplift	Osinskaya-3R	Q	0–5 m – sands, loams
		€m_3–€m_1	carbonate-terrigenous rocks (by analogy)
Irkutsk bench			
Belsky uplift	Belskaya-1	Q	0–20 m – sands
Irkutsk basin		€m_3–€m_1	dolomites, limestones, dolomitized limestones
Baikal rift zone			
Ust-Selenginsky basin	Baikalskaya-1	Q	0–237 m – gravels and pebbles
		Tr	237–1809 m – clays, sandy pebbles, aleurites, sandstones
		Pcm	1809–1825 m – quartzites, amphibolites, granites
	Baikalskaya-3	Q	0–228 m – sandy gravels
		Tr	228–2558 m – clays, sands, aleurolites
	Istokskaya-4	Q	0–96 m – sands, gravel, pebble
		N_2Pli	96–300 m – clay and sand
		N_2Mi	300–2802 m – intercalation of clay, sands, sandstones, aleurolites and argillites
Tunka basin	Tunkinskaya-2	$Q_4–Q_{2-3}$	0–430 m – sandy deposits
		$N_2–Q_1$	430–720 m – sands, sandstones, argillites, pebbles
		N_2	720–1200 m – sandstones, clayey sands, basalts
		N_1	1200–2100 m – aleurolites, sands, sandstones, basalts, coal slates

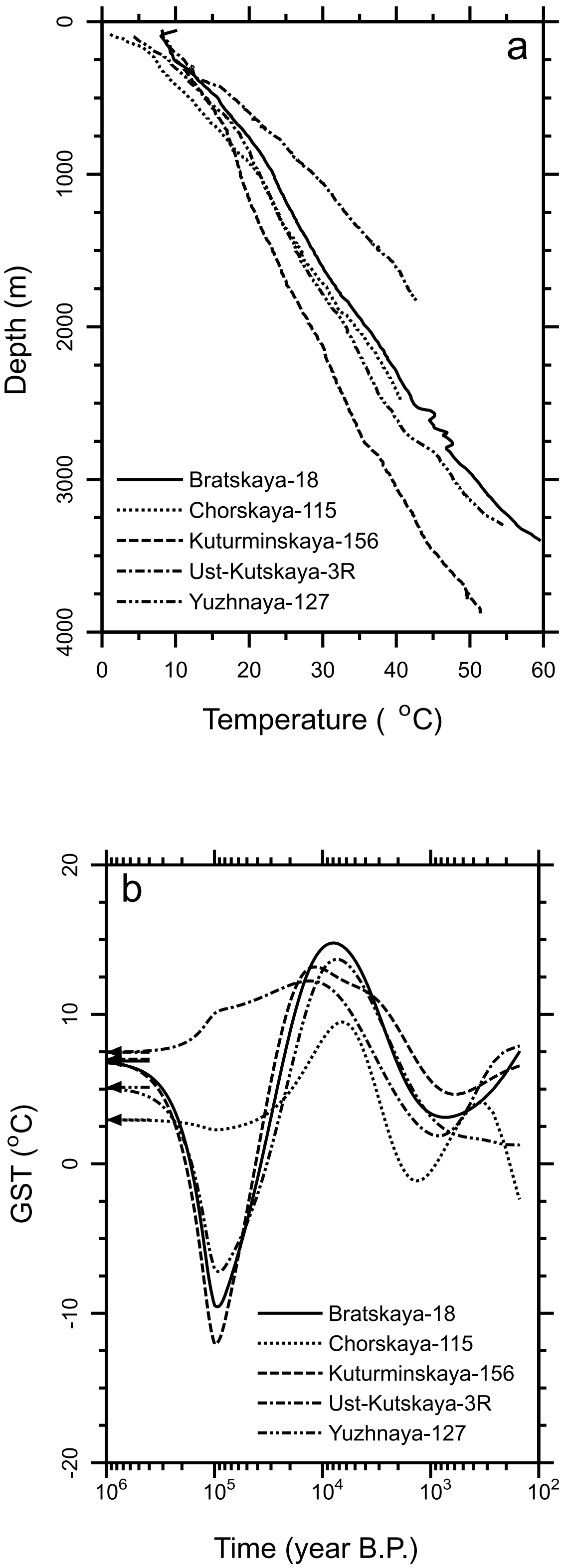

Fig. 3. (a) Temperature logs and (b) estimated GST histories for borehole sites of group 1, located within the Ust-Kutsky dome and zones of Angarsk dislocations and Angarsk syneclise.

cannot offer rigorous proof, but our inverse results suggest that drilling disturbances may significantly corrupt the estimates for the long-term mean GST, the basal HFD, and small-scale climate changes in the Holocene, but they do not dramatically corrupt the estimates for large-scale climate changes, such as the P/H transition. As has already been mentioned earlier, a plausible explanation is that drilling disturbances have a signature that differs significantly from that of the P/H transition, thus allowing us to suppress their adverse effects by imposing an a priori autocovariance for $V_s(t)$ that favors the retrieval of the P/H transition.

Geothermal parameters of the selected boreholes are typical of the south of the Siberian platform. The geothermal gradient varied from 10 to 17 (the average value is 13 ± 1) mK/m; rather high values for the thermal conductivity of the rocks (2.8–3.2 W/m/K) are due to the thick salt-bearing layers. Heat flow values vary from 32 to 50 mW/m^2, with an average of 39 ± 2 mW/m^2 [20]. The most significant anomalous feature occurs within the zone of the Angarsk dislocations, where the boreholes penetrate a thick sedimentary cover. Crustal temperatures vary dramatically in this zone. For example, the temperatures at the depth of 3500 m vary from 45°C at Kuturminskaya-156 to 60°C at Bratskaya-18.

We will divide the selected boreholes into three groups, from north to south, in accordance with their geographic (latitudinal) proximity, which also roughly coincides with a tectonic grouping. Geographic proximity is more relevant than tectonic setting insofar as climate change is concerned. Group 1, located within the Ust-Kutsky dome and zones of Angarsk dislocations, and Angarsk syneclise, consists of Bratskaya-18, Chorskaya-115, Kuturminskaya-156, Ust-Kutskaya-3R, and Yuzhnaya-127. Group 2, located within the zone of Verkhneangarsk dislocations, consists of Atovskaya-1, Atovskaya-9, Belskaya-1, Birkin-

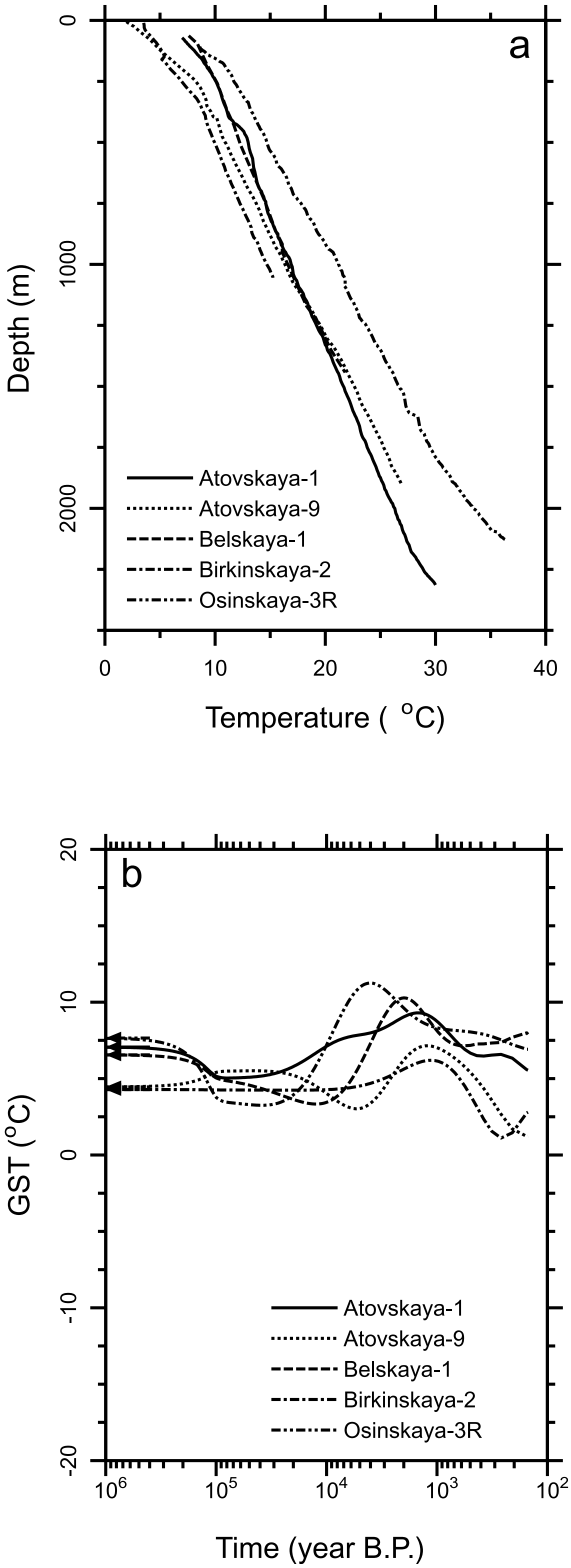

skaya-2, and Osinskaya-3R. Finally, group 3, located in the Baikal rift zone, consists of Baikalskaya-1, Baikalskaya-3, Istokskaya-4, and Tunkinskaya-2. The measured *T–z* profiles and the estimated GST histories for the three groups are shown in Figs. 3–5, respectively.

4. Discussion and conclusion

The most significant observation we can make on the results is the remarkable consistency in the timings of the P/H transition for all three groups. The long-term mean GSTs, on the other hand, vary significantly from site to site within each group despite their geographic proximity. This is an indication that drilling disturbances may have significantly affected the determination of the long-term mean GST but only to a limited extent on the timing of the P/H transition. We observe that the amplitudes of the P/H transition also vary from site to site in each group. However, the in-group amplitude variation is likely not real. For group 3, the amplitude variation among Baikalskaya-1, Baikalskaya-3, and Istokskaya-4, which are located very close together, may have been a consequence of the differing depth penetrations and data densities of the boreholes, and of the effects of drilling disturbances. The amplitude variation for group 1 is also questionable. For Chorskaya-115 and Ust-Kutskaya-3R, temperatures at the LGM are seen to be higher than the present temperature. This is a highly suspicious result. The *T–z* log for Chorskaya-115 was obtained only 3 days after drilling, and the drilling dates for Ust-Kutskaya-3R are not known. For these two boreholes, the effects of drilling disturbances may have been so severe as to invalidate our results. Excluding Chorskaya-115 and Ust-Kutskaya-3R, the amplitudes of the P/H transition for group 1 are consistent.

The second important observation of the results is a north to south variation in both the ampli-

←
Fig. 4. (a) Temperature logs and (b) estimated GST histories for borehole sites of group 2, located within the zone of Verkhneangarsk dislocations.

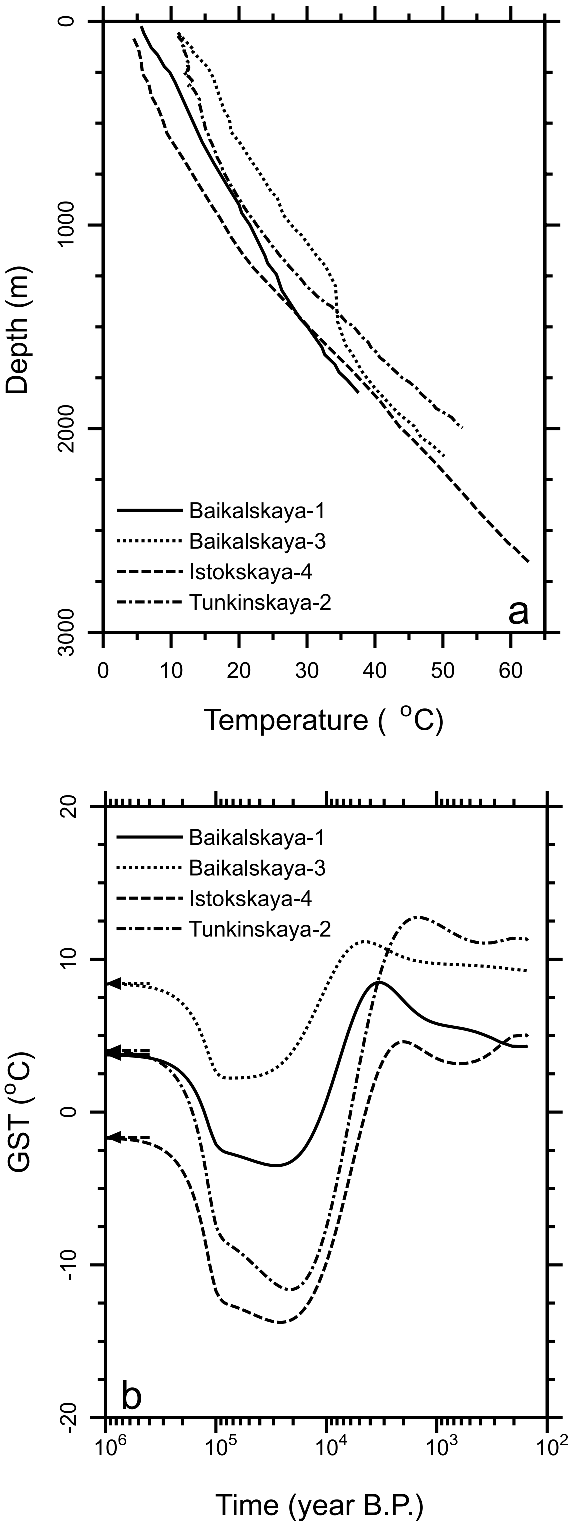

tude and timing of the P/H transition. The borehole sites in groups 1 and 3 show a distinctive P/H transition with a warming of about 25 K. On the other hand, the borehole sites in group 2 show a P/H warming of no more than 8 K. The subdued P/H warming for group 2 cannot be attributed to inadequate depth penetrations of the boreholes except for Birkinskaya-2, where *T–z* data are available only to a depth of 1055 m and for Belskaya-1, where data are available only to a depth of 1443 m. The other three boreholes are all sufficiently deep to resolve a substantial portion of the warming. The most plausible explanation for the north to south variation in the amplitude of the P/H transition is a corresponding north to south variation in the temperature at the base of the ice sheet, although effects of drilling disturbances and other non-climatic effects cannot be excluded as the cause without additional supporting evidence. It is known that temperatures at the base of an ice sheet can vary spatially. For example, temperatures at the base of the Greenland Ice Sheet are −8.58 and −13.22°C, respectively, for the GRIP (72.6°N, 37.6°W) and Dye-3 (65.2°N, 43.8°W) boreholes [17]. However, the implied north to south variations from group 1 to 2 and from group 2 to 3 are substantially greater than that between GRIP and Dye-3, especially considering the close proximity of the three groups.

We note that, although the amplitudes of the P/H transition are roughly the same (25 K) for groups 1 and 3, the timings and the durations are significantly different. For group 1, warming began as early as 90 ka and reached a maximum at about 7 ka. On the other hand, for group 3, warming did not begin until about 20 ka and reached a maximum at about 4 ka. The onset time of the P/H transition for group 3 is consistent with that found in the proxy records (diatom abundance and organic carbon $\delta^{13}C$) of the Lake Baikal sediment core BDP-93-2 [21,22]. It is also in general agreement with the onset times estimated from *T–z* data of the Ljutomer borehole

←
Fig. 5. (a) Temperature logs and (b) estimated GST histories for borehole sites of group 3, located within the Baikal rift zone and its southwestern flank.

in Slovenia [16], the GRIP borehole on the Greenland Ice Sheet [17], and the Sept-Iles borehole in Quebec, Canada [18]. The much earlier onset of warming for group 1 is problematical. It is tempting to attribute the early onset for group 1 to drilling disturbances, but the consistency of results for Bratskaya-18, Kuturminskaya-156, and Yuzhnaya-127 renders such an explanation questionable. Also problematical for group 1 is the extremely large (up to 8 K) cooling that follows the HM. The modest post-HM cooling of 1–3 K found for groups 2 and 3 is more consistent with proxy records and with other estimates from borehole *T*–*z* data, referred to above. In addition to the effects of drilling disturbances, a possible explanation for the unexpected results for group 1 is a severe misrepresentation of the thermal structure. However, such a misrepresentation is not suggested by the data available. Finally, we note that the P/H warming of 25 K for groups 1 and 3 is identical to the warming estimated for the GRIP borehole, but substantially higher than those estimated for Ljutomer (8 K) and Sept-Iles (11 K).

The presence of non-climatic systematic noise suggests that one should seek the mean for each group. If the effects of drilling disturbances are to some extent random from site to site, then a group mean would be a more robust estimate than the individual GST histories. The only drawback is that the group mean may underestimate the amplitude of the P/H transition because the extent to which this amplitude can be recovered depends on the depth penetration, which varies from site to site. The mean GST histories for the three groups, with the steady-state component U_s removed, are shown in Fig. 6. Also shown is the mean of the three groups. In computing the group means, two boreholes in group 1 (Chorskaya-115 and Ust-Kutskaya-3R) are excluded on the basis of possibly having excessive remanent drilling disturbances, two boreholes in group 2 (Belskaya-1 and Birkinskaya-2) are excluded on the basis of insufficient depth penetration. Baikalskaya-3 in group 3 is also excluded due of a break in the *T*–*z* profile at a depth of about 1500 m (Fig. 5a), possibly the result of waterflow or thermal conductivity contrast. Although the break has relatively short wavelengths, it compels us to relax the constraint imposed on the *T*–*z* data, resulting in an underestimate for the amplitude of the P/H transition. We compute the group mean by simultaneously inverting all *T*–*z* logs in each group [23], assuming that the borehole sites have a common $V_s(t)$. A simple arithmetic mean of the individual GST histories would also give essentially the same result [23]. Except for a relatively subdued amplitude for the P/H transition, the observations made above regarding the P/H transition apply to the group means.

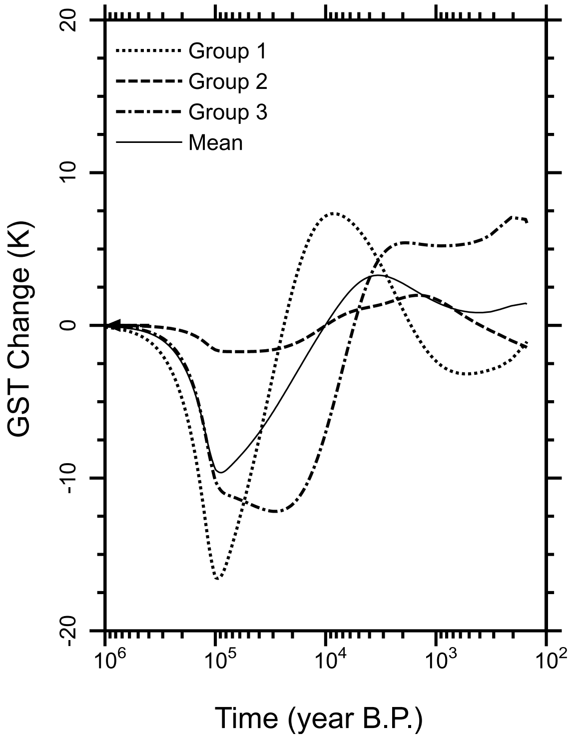

Fig. 6. Mean GST histories for groups 1, 2, and 3 and for the study area.

In FSI formulation, the basal HFD (Q_b) is estimated simultaneously with the GST history. The estimated basal HFDs, free of the climate changes shown in Figs. 3–5, and free of the heat production, are given in Table 1. Also given in parentheses are the mean interval HFDs, determined as the product of mean thermal conductivity and mean geothermal gradient. Except for Birkinskaya-2, the two values do not differ significantly, which shows that the product of mean thermal conductivity and geothermal gradient can give a reasonable estimate for the basal HFD in most cases. However, a simultaneous estimation of Q_b and the GST history allows for an optimal reduction of errors caused by inadequate borehole depth and by data noise.

We conclude with a short remark: The presence of drilling disturbances in the *T–z* data renders it questionable to use the data for climate reconstruction. Nevertheless, our results suggest that, even for data with such a poor quality, valuable information about large-scale climatic changes can still be retrieved. Our results are in gross agreement with those found in the proxy records (diatom abundance and organic carbon $\delta^{13}C$) of the Lake Baikal sediment core BDP-93-2 [21,22]. However, additional proxy records are needed to validate our results.

Acknowledgements

We thank Dr. D.Yu. Demezhko and an anonymous reviewer for their constructive reviews, T. Leshkevich for translations, and Prof. K.G. Levi, Dr. S.V. Lysak, Dr. Yu.B. Trzhitsinsky, Dr. V.I. Sizhykh, and Dr. A.A. Dzuba for their help.***[RV]***

References

[1] V.V. Bufal, N.N. Gustokashina, I.E. Trofimova, Ecological Risk, Materials of the 2nd All-Russian Conference, Irkutsk, 2001, pp. 199–201 (in Russian).

[2] P.D. Jones, K.R. Briffa, T.P. Barnett, S.F.B. Tett, High-resolution palaeoclimatic records for the last millennium: interpretation, integration and comparison with general circulation model control-run temperatures, Holocene 8 (1998) 455–471.

[3] M.E. Mann, R.S. Bradley, M.K. Hughes, Global-scale temperature patterns and climate forcing over the past six centuries, Nature 392 (1998) 779–787.

[4] J. Esper, E.R. Cook, F.H. Schweingruber, Low-frequency signals in long tree-ring chronologies for reconstructing past temperature variability, Science 295 (2002) 2250–2253.

[5] K.R. Briffa, T.J. Osborn, Blowing hot and cold, Science 295 (2002) 2227–2228.

[6] H.N. Pollack, S. Huang, P.Y. Shen, Climate change record in subsurface temperatures: a global perspective, Science 282 (1998) 279–281.

[7] H.N. Pollack, S. Huang, Climate reconstruction from subsurface temperatures, Annu. Rev. Earth Planet. Sci. 28 (2000) 339–365.

[8] S. Huang, H.N. Pollack, P.Y. Shen, Temperature trends over the past five centuries reconstructed from borehole temperatures, Nature 403 (2000) 756–758.

[9] R.P. Dorofeeva, GST-studies in the southern East Siberia and Mongolia, in: International Workshop 'Borehole, Temperatures and Climate Change', Prague, June 20–24, 1994, pp. 111–122.

[10] P.Y. Shen, A.E. Beck, Least squares inversion of borehole temperature measurements in functional space, J. Geophys. Res. 96 (1991) 19965–19979.

[11] P.Y. Shen, A.E. Beck, Paleoclimate change and heat flow density inferred from temperature data in the Superior Province of the Canadian Shield, Palaeogeogr. Palaeoclimatol. Palaeoecol. (Global Planet. Change Sect.) 98 (1992) 143–165.

[12] P.Y. Shen, K. Wang, H. Beltrami, J.-C. Mareschal, A comparative study of inverse methods for estimating climatic history from borehole temperature data, Palaeogeogr. Palaeoclimatol. Palaeoecol. (Global Planet. Change Sect.) 98 (1992) 113–127.

[13] G.D. Clow, The extent of temporal smearing in surface-temperature histories derived from borehole temperature measurements, Palaeogeogr. Palaeoclimatol. Palaeoecol. (Global Planet. Change Sect.) 98 (1992) 81–86.

[14] P.Y. Shen, H.N. Pollack, S. Huang, K. Wang, Effects of subsurface heterogeneity on the inference of climate change from borehole temperature data: model studies and field examples from Canada, J. Geophys. Res. 100 (1995) 6383–6396.

[15] S. Huang, H.N. Pollack, P.Y. Shen, Late Quaternary temperature changes seen in world-wide continental heat flow measurements, Geophys. Res. Lett. 24 (1997) 1947–1950.

[16] D. Rajver, J. Safanda, P.Y. Shen, The climate record inverted from borehole temperatures in Slovenia, Tectonophysics 291 (1998) 263–276.

[17] D. Dahl-Jensen, K. Mosegaard, N. Gundestrup, G.D. Clow, S.J. Johnsen, A.W. Hansen, N. Balling, Past temperatures directly from the Greenland Ice Sheet, Science 282 (1998) 268–271.

[18] J.-C. Mareschal, F. Rolandone, G. Bienfait, Heat flow variations in a deep borehole near Sept-Iles, Quebec, Canada: Paleoclimatic interpretation and implications for regional heat flow estimates, Geophys. Res. Lett. 26 (1999) 2049–2052.

[19] Yu.A. Zorin, Neostructure and Isostasy of the Baikal Rift Zone and Adjacent Areas, Nauka, Moscow, 1971, 168 pp. (in Russian).

[20] R.P. Dorofeeva, S.V. Lysak, Geothermal profiles of the lithosphere in Central Asia, Tectonophysics 164 (1989) 165–173.

[21] A.A. Prokopenko, D.F. Williams, E.B. Karabanov, G.K.

Khursevich, Response of Lake Baikal ecosystem to climate forcing and pCO_2 change over the last glacial/interglacial transition, Earth Planet. Sci. Lett. 172 (1999) 239–253.

[22] A.A. Prokopenko, E.B. Karabanov, M.I. Kuzmin, D.F. Williams, Factors of early glaciation in Siberia at transition from Kazantsevsky climatic optimum to Zyryanovsky glacial period (results of the study of bottom sediments of Lake Baikal), Geol. Geophys. 42 (2001) 1–2, 64–75 (in Russian).

[23] H.N. Pollack, P.Y. Shen, S. Huang, Inference of ground surface temperature history from subsurface temperature data interpreting ensembles of borehole logs, PAGEOPH 147 (1996) 537–550.